

# Nb<sub>3</sub>Sn COATING OF A 2.6 GHz SRF CAVITY BY SPUTTER DEPOSITION TECHNIQUE\*

M. S. Shakel<sup>†</sup>, W. Cao, H. E. Elsayed-Ali, Md. N. Sayeed, Old Dominion University, Norfolk, VA  
G. Ereemeev, Fermi National Accelerator Laboratory, Batavia, IL, USA  
U. Pudasaini, A. M. Valente-Feliciano  
Thomas Jefferson National Accelerator Facility, Newport News, VA, USA

## Abstract

Nb<sub>3</sub>Sn is considered promising as a coating for superconducting radio frequency (SRF) cavities due to its high transition temperature  $T_c \sim 18.3$  K and superheating field  $H_{sh} \sim 400$  mT, almost twice that of Nb. A cylindrical DC magnetron sputtering system was built, commissioned, and used to deposit Nb<sub>3</sub>Sn on the inner surface of a 2.6 GHz single-cell Nb SRF cavity. With two identical cylindrical magnetrons, this system can coat the cavity with high symmetry and uniform thickness. Using Nb-Sn multilayer sequential sputtering followed by annealing at 950 °C for 3 h, Nb<sub>3</sub>Sn films are first deposited at the equivalent positions of the cavity's beam tubes and the equator. The films' compositions and crystal structures are characterized by energy dispersive spectroscopy (EDS) and X-ray diffraction (XRD), respectively. The  $T_c$  of the films are measured by the four-point probe method and are observed to be 17.61 to 17.76 K. Based on these studies,  $\sim 1.2$   $\mu\text{m}$  thick Nb<sub>3</sub>Sn is deposited inside a 2.6 GHz SRF Nb cavity. We discuss the first results from samples and cavity coatings and the operation of the cylindrical sputtering system.

## INTRODUCTION

Compared to Nb SRF cavities, Nb cavities coated with Nb<sub>3</sub>Sn can achieve high-quality factors at 4 K and can replace the bulk Nb cavities operated at 2 K, hence reducing the operation cost significantly [1-4].

One of the methods used to deposit Nb<sub>3</sub>Sn coating on Nb SRF cavities is Sn vapor diffusion [5-7]. Magnetron sputtering is another promising method for Nb<sub>3</sub>Sn coating as it provides better control over stoichiometry than the Sn diffusion process [8]. Magnetron sputtering is applied in several methods to grow Nb<sub>3</sub>Sn: Depositing multilayers of Nb-Sn followed by annealing, from a single stoichiometric Nb<sub>3</sub>Sn target, or by co-sputtering of Nb and Sn [9-13].

We have commissioned a cylindrical DC magnetron sputtering system at Old Dominion University to coat the inside surface of a 2.6 GHz Nb SRF cavity with Nb<sub>3</sub>Sn. By applying multilayer sequential sputtering to deposit Nb-Sn layers using the two identical magnetrons followed by annealing, Nb<sub>3</sub>Sn thin film is grown on Nb at the equivalent positions of the 2.6 GHz SRF cavity beam tubes and the equator.

\* Supported by DOE, Office of Accelerator R&D and Production, Contact No. DE-SC0022284, with partial support by DOE, Office of Nuclear Physics DE-AC05-06OR23177, Early Career Award to G. Ereemeev.

<sup>†</sup> mshak001@odu.edu

## DESIGN OF CYLINDRICAL DC MAGNETRON SPUTTER COATER

The cylindrical magnetron sputtering system, schematically shown in Fig. 1, consists of the custom-designed high vacuum deposition chamber and two identical cylindrical magnetrons, designed and built by PLASMIONIQUE Inc. that can travel inside the cavity while depositing Nb or Sn.

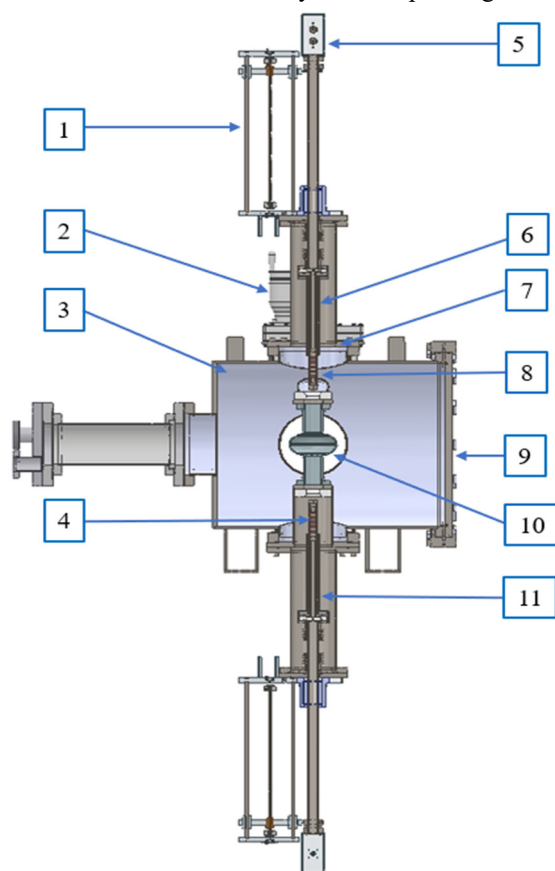


Figure 1: A sketch of the cylindrical DC magnetron sputtering system: (1) Magnetron movement controller shaft, (2) Gate valve, (3) Vacuum chamber, (4) Magnets, (5) Water flow controller, (6) Top magnetron, (7) 8" ConFlat (CF) port of top magnetron, (8) Tube target, (9) Chamber door, (10) 2.6 GHz Nb SRF cavity, (11) Bottom magnetron; The magnetrons are made by PLASMIONIQUE Inc to fit an ODU custom chamber.

The coating chamber is designed to accommodate a 2.6 GHz TESLA-shaped cavity and two vertically positioned cylindrical magnetrons. The magnetrons are inserted into the chamber and placed on the axis of the cavity through two 8" CF flange ports, one from the top and the other from the bottom of the chamber.

Each cylindrical magnetron has 4 separate ring magnets made of neodymium (N55 grade) and coated with Ni, Cu, and epoxy. All magnets have the same diameter (OD 16 mm × ID 4 mm), though the two outer magnets are longer (7.74 mm) than the two middle magnets (6.35 mm). The magnetic field of these magnets creates 4 ring-shaped plasma formations around the target. Water-cooling through the magnetrons keeps the magnets cool.

Customized software is used to operate the associated devices connected with the cylindrical sputter system, including a communication device for magnetron selection, a motor control device for magnetron movement, and a DC power supply. The software can operate a deposition program and store readings of current, voltage, power, and water flow rate during deposition.

### MAGNETRON OPERATION

The magnetron discharge operating conditions that produce stable and symmetric plasma for the Nb and Sn targets were identified. Individual tube targets of Nb and Sn with identical dimensions (0.9" OD × 0.8" ID × 4.5", 99.99% purity from ACI ALLOYS Inc.) were installed on the top magnetron and bottom magnetron, respectively. The chamber was pumped to  $\sim 8 \times 10^{-8}$  Torr. Then, Ar was introduced at the 10 mTorr deposition pressure with a flow rate of 50 SCCM.

For a DC power of  $\geq 18$  W, symmetric plasma rings form around the Nb target. Fig. 2(a) shows stable plasma formation around the Nb target obtained at 30 W DC power. Two outer plasma rings are visibly more intense than the two weaker middle plasma rings.

Due to the much lower melting temperature of Sn (231.9 °C) compared to Nb (2469 °C) and its higher sputter yield, lower DC power is applied to the Sn target. Operating the Sn discharge at 8 W produces 4 plasma rings around the target; the outer 2 plasma rings are brighter than the 2 middle plasma rings, as visible in Fig. 2(b).

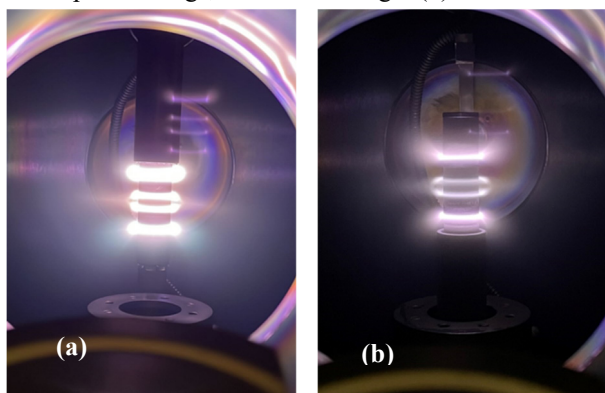


Figure 2: Plasma discharge using a DC power supply (a) Nb at 30 W, (b) Sn at 8 W.

## MULTILAYER SEQUENTIAL SPUTTER DEPOSITION

A custom-made sample holder is used to mount 3 Nb substrates ( $10 \times 10 \times 3$  mm<sup>3</sup>) with the location of their surfaces replicating the inner surface of the 2.6 GHz Nb SRF cavity equator and irises. Nb and Sn are sputtered by applying 30 and 8 W DC power, respectively. For desired thicknesses of Nb and Sn, the speed of the magnetron movement and the number of scans are adjusted. A 200-nm thick Nb buffer layer is deposited on Nb substrate. Then, multi-layers of 25 nm thick Sn and 50 nm thick Nb are sequentially deposited. A total of 16 layers of Nb and Sn are deposited. For the 25 nm thick Sn layer, the Sn target travels across the deposition region once at a speed of 0.75 mm/s, and for the 50 nm thick Nb layer, the Nb target travels twice across the same region at a speed of 1 mm/s. The thickness of the films on the equator and the top and bottom beam tubes were 1200, 880, and 824 nm, respectively, as measured by a cross-sectional scanning electron microscope image. The samples are annealed at 950 °C for 3 h in a separate furnace with a temperature ramp rate of 12 °C/min.

### RESULT AND DISCUSSION

The elemental compositions of Nb and Sn of the as-deposited and annealed samples are listed in Table 1. The as-deposited samples from the three positions have Sn atomic compositions of 25–33%. The annealed sample from the top beam tube position has an Sn composition of ~22%, while samples placed at the equator and bottom beam tube positions have ~19% Sn. This loss of Sn in the annealing process was observed before [8].

Table 1: Composition of Sn in As-deposited and Annealed Samples

Positions	Sn composition of as-deposited samples (at.%)	Sn composition of annealed samples (at.%)
Top beam tube	33	22
Equator	32	19
Bottom beam tube	25	19

The XRD patterns of the as-deposited and annealed samples are shown in Fig. 3. All three as-deposited samples show multiple Nb diffraction peaks ((110), (200), (211), (310)) coming from the substrates and the films. The top beam tube position sample shows several Sn diffraction peaks ((200), (101), (220), (211), (112), and (400)).

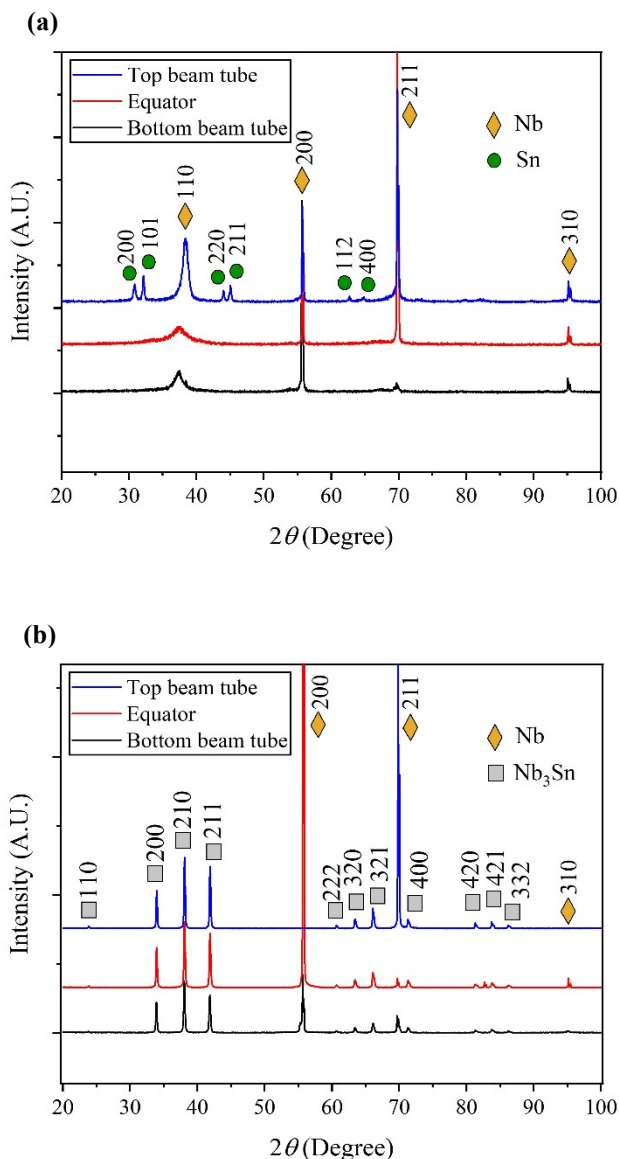


Figure 3: XRD patterns of (a) Nb-Sn as-deposited samples, (b) annealed Nb<sub>3</sub>Sn samples.

The formation of Nb<sub>3</sub>Sn after annealing is verified from the XRD patterns. Annealed samples from all three positions show several diffraction peaks corresponding to Nb<sub>3</sub>Sn (110), (200), (210), (211), (222), (320), (321), (400), (420), (421), and (332). No diffraction peaks corresponding to Nb and other Nb-Sn intermetallic phases other than Nb<sub>3</sub>Sn are observed, which confirms that the thin film is Nb<sub>3</sub>Sn only. Several Nb peaks ((200), (211), (310)) are observed in the annealed films that are coming from the substrate.

The superconducting critical temperature transition width ( $\Delta T_c$ ) and residual resistivity ratio (RRR) of the annealed samples are measured by the four-point probe method down to 4 K [14]. Figure 4 shows the changes in resistivity with temperature and the inset image shows the superconducting transition region of the films.

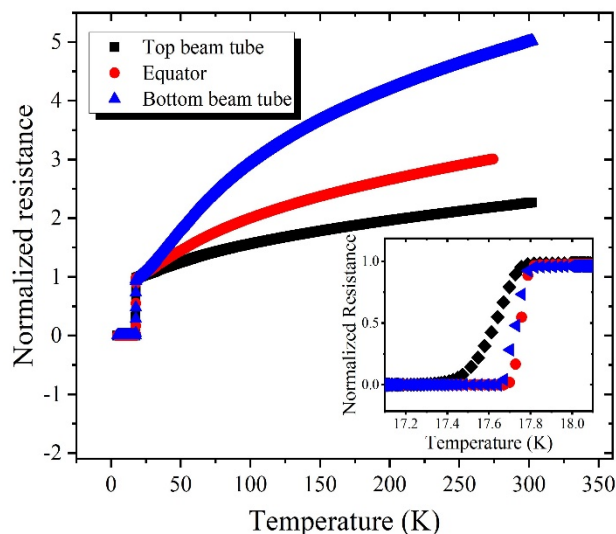


Figure 4: Sample resistance with temperature. Note that Nb<sub>3</sub>Sn films were deposited on sapphire and the resistance was measured by a four-point probe method.

For all three samples, the Nb<sub>3</sub>Sn films have  $T_c$ ,  $\Delta T_c$ , and RRR in Table 2. The highest  $T_c$  of 17.76 K and lowest  $\Delta T_c$  of 0.06 K are observed for the film at the equator location.

Table 2: Superconducting Properties of the Nb<sub>3</sub>Sn Films

Positions	$T_c$ (K)	$\Delta T_c$ (K)	RRR
Top beam tube	17.61	0.24	2.26
Equator	17.76	0.06	3.00*
Bottom beam tube	17.73	0.1	5.01

\* The RRR value for the sample at the equator position is measured from the ratio of the resistance at 275 K to that at 20 K. The other RRR value is measured from the ratio of resistance at 300 K to that at 20 K.

## SUMMARY

We have commissioned a cylindrical DC magnetron sputtering system and used it to deposit Nb<sub>3</sub>Sn films on flat samples at equivalent positions of equator and beam tubes of a 2.6 GHz Nb SRF cavity. The samples had  $T_c$  of 17.61–17.76 K and  $\Delta T_c$  of 0.06–0.24 K. We have also coated an SRF cavity using the same conditions as used to coat the flat test samples. The cavity testing is in progress.

## REFERENCES

- [1] A. M. Valente-Feliciano, “Superconducting RF materials other than bulk niobium: a review”, *Supercond. Sci. Technol.*, vol. 29, no. 11, p. 113002, Sep. 2016. doi:10.1088/0953-2048/29/11/113002
- [2] S. Posen and D. L. Hall, “Nb<sub>3</sub>Sn superconducting radiofrequency cavities: Fabrication, results, properties, and prospects”, *Supercond. Sci. Technol.*, vol. 30, p. 033004, pp. 2017. doi:10.1088/1361-6668/30/3/033004

- [3] U. Pudasaini, G. V. Ereemeev, C. E. Reece, J. Tuggle, and M. J. Kelley, "Initial growth of tin on niobium for vapor diffusion coating of Nb<sub>3</sub>Sn", *Supercond. Sci. Technol.*, vol. 32, p. 045008, Mar. 2019.  
doi:10.1088/1361-6668/aafa88
- [4] U. Pudasaini *et al.*, "Recent Results From Nb<sub>3</sub>Sn Single Cell Cavities Coated at Jefferson Lab", in *Proc. SRF'19*, Dresden, Germany, Jun.-Jul. 2019, pp. 65-70.  
doi:10.18429/JACoW-SRF2019-MOP018
- [5] G. Ereemeev *et al.*, "Nb<sub>3</sub>Sn multicell cavity coating system at Jefferson Lab", *Rev. Sci. Instrum.*, vol. 91, no. 7, Jul. 2020. doi: 10.1063/1.5144490
- [6] S. Posen *et al.*, "Nb<sub>3</sub>Sn at Fermilab: Exploring Performance", in *Proc. SRF'19*, Dresden, Germany, Jun.-Jul. 2019, pp. 818-822.  
doi:10.18429/JACoW-SRF2019-THFUB1
- [7] S. Posen, M. Liepe, D.L. Hall, "Proof-of-principle demonstration of Nb<sub>3</sub>Sn superconducting radiofrequency cavities for high Q0 applications", *Appl. Phys. Lett.*, vol. 106, no. 8, Feb. 201. doi:10.1063/1.4913247
- [8] M. N. Sayeed, U. Pudasaini, C. E. Reece, G. V. Ereemeev, and H. E. Elsayed-Ali, "Effect of layer thickness on structural, morphological and superconducting properties of Nb<sub>3</sub>Sn films fabricated by multilayer sequential sputtering," in IOP Conf. Ser.: Mater. Sci. Eng., Jun. 2020, vol. 756, p. 012014. doi: 10.1088/1757-899X/756/1/012014
- [9] Md. N. Sayeed *et al.*, "Deposition of Nb<sub>3</sub>Sn Films by Multilayer Sequential Sputtering for SRF Cavity Application", in *Proc. SRF'19*, Dresden, Germany, Jun.-Jul. 2019, pp. 637-641. doi:10.18429/JACoW-SRF2019-TUP079
- [10] E. A. Ilyina *et al.*, "Development of sputtered Nb<sub>3</sub>Sn films on copper substrates for superconducting radiofrequency applications," *Supercond. Sci. Technol.*, vol. 32, no. 3, 2019. doi:10.1088/1361-6668/aaf61f
- [11] M. N. Sayeed, U. Pudasaini, C. E. Reece, G. V. Ereemeev, and H. E. Elsayed-Ali, "Properties of Nb<sub>3</sub>Sn films fabricated by magnetron sputtering from a single target", *Appl. Surf. Sci.*, vol. 541, pp. 148528, Mar. 2020. doi: 10.1016/j.apsusc.2020.148528
- [12] R. Valizadeh *et al.*, "PVD Deposition of Nb<sub>3</sub>Sn Thin Film on Copper Substrate from an Alloy Nb<sub>3</sub>Sn Target", in *Proc. IPAC'19*, Melbourne, Australia, May 2019, pp. 2818-2821. doi:10.18429/JACoW-IPAC2019-WEPRB011
- [13] C. Sundahl, "Synthesis of Superconducting Nb<sub>3</sub>Sn Thin Film Heterostructures for the Study of High-Energy RF Physics, PhD Dissertation, University of Wisconsin-Madison, Wisconsin, USA, 2019.
- [14] J. J. K. Spradlin, C. E. Reece, and A-M. Valente-Feliciano, "A Multi-Sample Residual Resistivity Ratio System for High Quality Superconductor Measurements", in *Proc. SRF'15*, Whistler, Canada, Sep. 2015, paper TUPB063, pp. 726-730. 1